Environ. Sci. Technol. **2006**, *40,* 4782−4787

Decomposition of Hydrogen Peroxide Driven by Photochemical Cycling of Iron Species in Clay

WENJING SONG, MINGMING CHENG, JIAHAI MA, WANHONG MA, CHUNCHENG CHEN, AND JINCAI ZHAO*

Key Laboratory of Photochemistry, Center for Molecular Science, Institute of Chemistry, Chinese Academy of Sciences, Beijing 100080, China

The reactivity of iron-bearing clays to catalyze the decomposition of hydrogen peroxide (H_2O_2) under light irradiation was investigated. Free iron oxides and structural iron in clay octahedral lattice are contained simultaneously in montmorillonite K10 (MK10), a representative natural clay mineral. By pretreatment of clay with the particular method, the reactivities of the two kinds of iron species were differentiated. It was found that free iron oxides on clay surface efficiently catalyzed the decomposition of H_2O_2 under UV light irradiation but structural iron in the octahedral lattice showed poor reactivity. This was found to result from the difference in production of Fe(II) species under UV irradiation between iron oxides and structural iron. When photoreactive substances such as *N,N*-dimethylaniline (DMA), rhodamine B (RhB), or malachite green (MG) were introduced, structural iron was found to promote greatly the decomposition of H_2O_2. The reduction of clay iron(III) to iron(II) is essential for the decomposition of H_2O_2, which is achieved by light-induced ligand to metal charge transfer (for iron oxides) or organic matters donating electrons upon irradiation (for structural iron). The light-induced redox cycling of iron did not lead to the release of iron and decomposition of H_2O_2 primarily localized on the clay surface. This work implies that iron-bearing clays could be a sink of H_2O_2 in the environmental system.

Introduction

Hydrogen peroxide (H_2O_2) is widely spread in natural waters and water/solid interfaces (*1*−*5*). Its decomposition is always accompanied by the generation of highly reactive oxygen species, and this process could have significant impact on the transformation of organic and inorganic species (*3*, *6*−*10*).

Various iron species were evidenced to contribute to the decomposition of H_2O_2, as well as the generation of free radicals or other reactive intermediates in the environment (*6*−*12*). The Haber−Weiss cycle (eqs 1−4) is one primary H_2O_2 decomposition route catalyzed by iron species, where ≡Fe(II) and ≡Fe(III) represent the Fe(II)/Fe(III) species in solid or solution phase. In acidic medium (pH < 4), ferrous and ferric ions in solution phase are responsible for the loss of H_2O_2; different kinds of iron oxides, such as goethite, hematite, magnetite, and ferrihydrite, are among the most ubiquitous forms of iron species under environmental relative conditions (pH 4−9) (*7*−*10*). They show quite different catalytic activity due to the surface area or valence of iron (*8*). Usually the decomposition of H_2O_2 primarily takes place on the surface active sites of these oxides (*8*−*10*). In the presence of natural ligands (oxalate, humic acid, et al.), however, iron is likely to be released from the oxide surface, increasing the contribution of solution phase reaction to the loss of H_2O_2 (*4*, *7*, *13*).

$$\equiv Fe(II) + H_2O_2 \rightarrow \equiv Fe(III) + {}^{\bullet}OH + OH^- \quad (1)$$

$$\equiv Fe(III) + H_2O_2 \rightarrow \equiv Fe(II) + O_2^{\bullet-}/HO_2^{\bullet} \quad (2)$$

$$\equiv Fe(III) + O_2^{\bullet-}/HO_2^{\bullet} \rightarrow \equiv Fe(II) + O_2 \quad (3)$$

$$\equiv Fe(II) + O_2^{\bullet-}/HO_2^{\bullet} \rightarrow \equiv Fe(III) + H_2O_2 \quad (4)$$

Previous investigations suggest that the reduction of ≡Fe(III) to ≡Fe(II) (eq 2) is the rate-limiting step in the overall reaction because the reaction of ≡Fe(II) with H_2O_2 is much faster than that of ≡Fe(III). Light irradiation and the presence of natural organic matters (NOM) could facilitate this process (*4*, *14*−*18*): (1) Fe(II) can be produced directly from the photolysis of photoreactive Fe(III) species, such as $Fe(OH)^{2+}$ and Fe(III) complexes with oxalic or humic acid (eq 5, L = inorganic or organic ligand for Fe(III)). (2) Some NOM can be excited by solar irradiation and donate electrons to Fe(III) species (eq 6). Therefore, the decomposition of H_2O_2 can be promoted by factors that assist conversion from Fe(III) to Fe(II). The reaction of (photo)produced Fe(II) with H_2O_2 has been reported to be an important source of •OH in systems composed of ferrihydrite/fulvic acid or iron loaded humic acid (*12*, *16*). In our previous work, it was found that quinones and dyes could reduce ferric ions and Fe(III) loaded on resins, accelerating significantly the decomposition of H_2O_2 and the removal of organic pollutants under visible irradiation (*19*−*22*).

$$\equiv Fe(III)L \xrightarrow{h\nu} \equiv Fe(II) + L^{\bullet} \quad (5)$$

$$NOM/NOM^* + Fe(III) \rightarrow \equiv Fe(II) + NOM^{\bullet+} \quad (6)$$

Clay minerals are widespread layer type aluminosilicates in the environment that are found on the earth's surface and in atmospheric aerosols in the stratosphere (*23*−*26*). Montmorillonite is a representative clay mineral, which is composed of units made up of two silica tetrahedral sheets and an alumina octahedral sheet (*23*). They could contain simultaneously iron species with different chemical environments: (1) free iron oxides that distribute randomly on clay surface; (2) structural iron that substitutes aluminum in the octahedral lattice; (3) iron complexed by surface hydroxyl groups on the edge of a clay sheet (complexed iron) (*23*, *27*, *28*). Structural iron in the octahedral clay lattice is of different chemical environment from that of the iron oxides. It is also an reactive electron-transfer center for many environmental processes: structural Fe(II) in ferruginous smectite could reduce the $-NO_2$ group of nitroaromatic compounds to an $-NH_2$ group (*27*, *28*); some bacteria reduce structural Fe(III) to Fe(II) during their respiration (*26*). Electrodes modified with iron-bearing clay could catalyze the electrochemical decomposition of H_2O_2. The reduction of Fe(III) to Fe(II) by electrochemically generated $MV^{\bullet+}$ was supposed to be the key step (*29*, *30*). This work tried to study the photocatalytic activity of iron species in clay for decomposition of H_2O_2. Using montmorillonite K10 as the representative clay, the photochemical reactivities of the two main iron species in it, free iron oxides and structural iron, were differentiated.

* Corresponding author phone: 86-10-8261-0080; fax: +86-10-8261-6495; e-mail: jczhao@iccas.ac.cn.

10.1021/es060624q CCC: $33.50
Published on Web 07/01/2006

In comparison with free iron oxides, structural Fe(III) showed poor activity under UV irradiation, which was ascribed to structural Fe(II) being hard to be produced upon UV irradiation. By introduction of particular photoreactive organic species, however, structural Fe(II) can be produced through electron injection by excited organics under UV or visible light, and the decomposition of H_2O_2 was promoted greatly. By dissolved iron measurement and other control experiments, it was evidenced that the redox cycling of both iron oxides and structural iron did not cause significant dissolution of iron and the solution phase reaction had insignificant contribution to the decomposition of H_2O_2 in the irradiated systems.

Experimental Section

Chemicals. Horseradish peroxidase (POD) was purchased from Huamei Biologic Engineering Co. (China). *N*,*N*-Diethyl-*p*-phenylenediamine (DPD) and 5,5-dimethyl-1-pyrroline-*N*-oxide (DMPO) were from Sigma. H_2O_2 (30 wt %), potassium phosphate monobasic (KH_2PO_4), sodium phosphate dibasic (Na_2HPO_4), sodium phosphate monobasic (NaH_2PO_4), ethylenediaminetetraacetic acid (EDTA), trisodium citrate, sodium bicarbonate, sodium dithionate, potassium chloride, hydrochloric acid, cetyltrimethylammonium bromide (CTAB), *N*,*N*-dimethylaniline (DMA), Rhodamine B (RhB), Malachite green (MG), and Ferrozine were of reagent grade and used without further purification. Barnstead UltraPure water (18.3 MΩ) was used throughout the study.

Minerals. Montmorillonite K10 with cation exchange capacity (CEC) of 100 mequiv/100 g was purchased from Aldrich. Laponite was kindly provided by Dr. H. Y. Zhu, Australian Key Centre of Microanalysis & Microscopy and School of Chemistry, The University of Sydney.

Organic impurities in the raw clay were oxidized with 2 M H_2O_2 at 80 °C (*31*), and then the clay was thoroughly washed and air-dried. The obtained sample (abbreviate as MK10) contained free iron oxides, structural iron, and complexed iron (the interlayer cation was K^+ as determined by X-ray photoelectron spectra (XPS)). Free iron oxides in MK10 were removed with trisodium citrate and sodium dithionate in sodium bicarbonate solution (CBD method, which only removes free iron oxides but not iron in the octahedral lattice; the structural Fe(III) can be reduced to structural Fe(II) in this process) (*31*, *32*). Briefly, 1 g of raw MK10 was added to a 50 mL solution of 0.3 M sodium citrate, 0.1 M sodium bicarbonate, and 0.1 M sodium dithionate, and the dispersion was shaken at 80 °C. The obtained sample was treated with 2 M H_2O_2 at 80 °C to remove organics and reoxidize structural Fe(II) to Fe(III). Then the clay was suspended in 1 M KCl solution (pH ~ 3) and stirred for 12 h for four times to ensure the sufficient intercalation of K^+ and removal of carbonate. Finally it was cleaned, centrifuged, and air-dried at 80 °C for 12 h. The sample was named as C-MK10, which contained structural iron and complexed iron but was free of iron oxides. The content of total iron in each sample was determined by JT-ULTIMA inductively coupling plasma-atomic emission spectra (ICP-AES) after digestion by concentrated acid, as displayed in Table S1 (Supporting Information).

Procedure and Analysis. The UV irradiation source was a 100 W Hg lamp (Toshiba SHL-100UVQ-2). Pyrex vessels were used as reactors so as to eliminate any irradiation below 300 nm. A 500 W halogen lamp acted as the visible irradiation source. (Irradiation below 450 nm was cut off by a light filter.)

The reaction suspensions contained a 0.2 g/L clay sample and 40 μM H_2O_2. The pH of the suspensions was adjusted to 5.0 ± 0.1 by dilute $HClO_4$ and NaOH. At a given time interval, about a 5 mL aliquot was sampled and centrifuged. The concentration of H_2O_2 in the supernatants was determined spectrophotometrically by the DPD method (*33*) on a Hitachi U-3100 spectrophotometer. Dissolved iron was determined by the Ferrozine method after the supernatants was filtered through a 0.2 μm filter (*34*). Samples for fluorescence experiments contained 0.04 g/L clay and 1 μM RhB. The exciting wavelength was 510 nm, and the fluorescence emission spectra were recorded on a Hitachi F-4500 spectrofluorometer. Electron paramagnetic resonance (EPR) signals of radicals trapped by DMPO were recorded at ambient temperature on a Brucker E500 spectrometer. The irradiation source was a Quanta-Ray Nd:YAG pulsed laser system (λ = 355 nm or 532 nm). The settings for the EPR spectrometer were the following: center field, 3480 G; sweep width, 100 G; microwave frequency, 9.64 GHz; modulation frequency, 100 kHz; power, 12 mW.

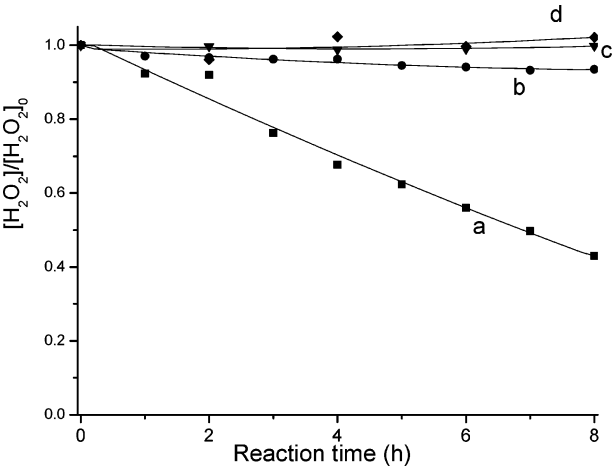

FIGURE 1. Variation in H_2O_2 concentration (a) in the presence and (b) in the absence of MK10 under UV irradiation, (c) in the presence of MK10 in the dark, and (d) in the presence of Laponite under UV irradiation. Initial conditions of reaction systems: MK10 = 0.2 g/L; Laponite = 0.2 g/L; H_2O_2 = 40 μM; pH 5.0.

Result and Discussion

UV Light Induced Decomposition of Hydrogen Peroxide Catalyzed by Montmorillonite K10. H_2O_2 was relatively stable under irradiation above 300 nm. However, in the presence of 0.2 g/L MK10, over a 50% decrease in H_2O_2 concentration was observed within 8 h (Figure 1). Such an effect of MK10 was primarily attributed to its photoreactivity because the loss of H_2O_2 in the dark was negligible (Figure 1, curve c).

Laponite is a synthetic counterpart of natural hectorite clay (magnesiansilicates) which has a microstructure similar to that of montmorillonite. Its effect on the decomposition of H_2O_2 was also examined, and there was almost no reduction in H_2O_2 concentration (Figure 1, curve d). A remarkable difference between MK10 and Laponite is the content of active metal, such as iron (*24*). This was confirmed by 1.99% and 0.01% of iron in MK10 and Laponite, as determined by ICP-AES (Table S1). Moreover, introduction of phosphate/EDTA, which form photoinert/photoreactive complexes with iron (*18*, *35*), greatly inhibited/accelerated the H_2O_2 decomposition (Supporting Information Figure S2), confirming the important role of iron in the reaction system.

Difference in Catalytic Activity between Each Type of Iron Species in Clay. To differentiate the reactivity of iron oxides and structural iron, original MK10 was treated according to the reported methods. After the clay sample was treated with the CBD procedure, free iron oxides were extracted into the solution phase. Then the dispersion was centrifuged, the precipitate was washed for further treatment, and the supernatants were collected. In the supernatants, not only iron (originates from iron oxides) but also Si, Al, and K (components of clay or SiO_2, Al_2O_3 impurities) were detected in the supernatants, indicating that other constitutes or

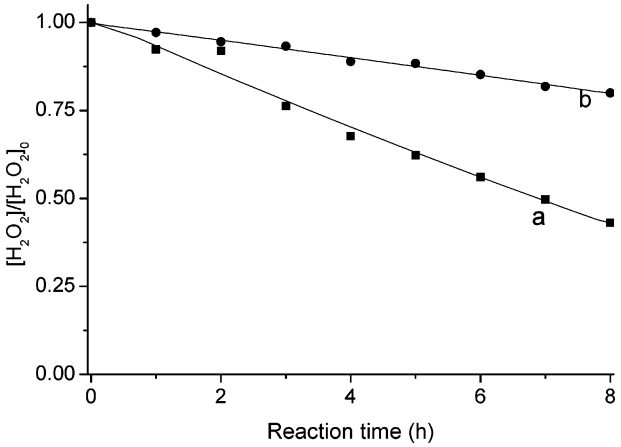

FIGURE 2. Decomposition of H_2O_2 in the presence of 0.2 g/L (a) MK10 and (b) C-MK10 (H_2O_2 = 40 μM, pH = 5.0).

TABLE 1. Concentration of Fe(II) in HCl Extraction after Irradiation of Various Dispersions (Clay, 1 g/L; RhB, 2.0 × 10^{-5} M; MG, 4.0 × 10^{-5} M; DMA, 1.0 × 10^{-4} M)

	MK10	C-MK10	C-MK10/ RhB	C-MK10/ MG	C-MK10/ DMA
irradiatn source	UV	UV	vis	vis	vis
Fe(II) (mM)	11	0.4	4.2	2.5	2.2

impurities of the clay might be removed during the treatment process. This means that the mass of both iron and clay decreased, and the reduction in the latter may be higher than that in the former. As a result, iron content (the mass ratio of iron to total clay) of C-MK10 was not very different from that of MK10 (2.05% and 1.99%, respectively; Table S1).

Free iron oxides accounted for about 15% of iron in clay (Supporting Information, calculation of free oxide amount in clay). Removal of this part of iron, as shown in Figure 2, resulted in great deceleration of H_2O_2 decomposition: about 57% of the H_2O_2 was decomposed after 8 h irradiation in the presence of MK10. However, in the case of C-MK10, 80% of H_2O_2 still remained under the same conditions. Considering that the edge area of montmorillonite accounts for a very small proportion of the total surface area (*36*), the percentage of iron complexed by surface hydroxyl group (complexed iron) is much lower than that of structural iron. Therefore, structural iron was responsible for the poor photocatalytic activity of C-MK10.

Since Fe(II) species have been evidenced to be necessary for H_2O_2 decomposition (*8*, *10*, *12*, *16*, *29*, *30*), the production of Fe(II) in clay samples under UV irradiation was examined to understand the difference in reactivity between iron oxides and structural iron. Briefly, 5 mL dispersions of MK10 and C-MK10 were prepared. They were deaerated with argon and stirred for 4 h under UV irradiation. Then 5 mL of HCl (1 M) free of oxygen was added and the resulting suspensions were allowed to react for 1 h to extract iron in the clay samples. The concentration of Fe(II) was determined in the supernatants after centrifugation. The photoproduced Fe(II) in MK10 was 11 μM, much higher than that in C-MK10 (0.4 μM, Table 1). In the case of iron oxides, Fe(II) could be produced through photolysis of ≡Fe(III)−OH, the surface form of iron oxides in aqueous solution (eq 7) (*10*, *37*, *38*). In contrast, structural Fe(III) in the octahedral lattice is sandwiched by two silica tetrahedral sheets and has little possibility to form photoreactive complexes with OH^-. As a result, structural Fe(III) shows poor activity to catalyze H_2O_2 decomposition.

$$\equiv Fe^{III}OH \xrightarrow{h\nu} \equiv Fe(II) + {}^{\bullet}OH \qquad (7)$$

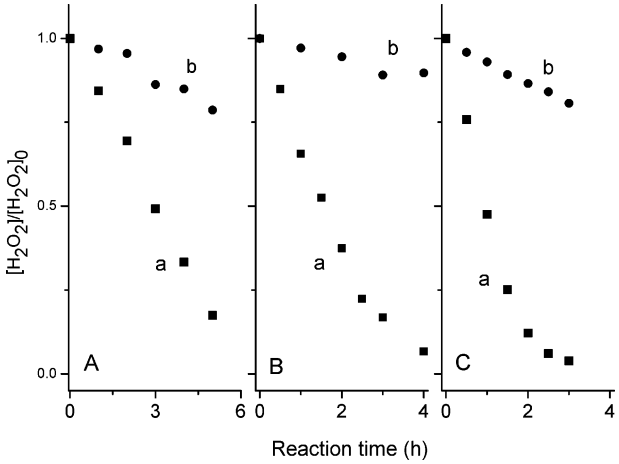

FIGURE 3. Variation in H_2O_2 concentration in reaction systems: (a) 0.2 g/L C-MK10 and organic species; (b) organic species. The organics were (A) 1.0 × 10^{-4} M DMA, (B) 2.0 × 10^{-5} M RhB, and (C) 4.0 × 10^{-5} M MG. Other conditions: H_2O_2 = 40 μM; pH = 5.0.

Structural Iron-Assisted Decomposition of H_2O_2 in the Presence of Photoreactive Substances under UV or Visible Irradiation. Our previous studies showed that some organic dyes at their excited states could facilitate the production of Fe(II) species by donating electrons to aqueous Fe^{3+} ions or Fe(III) supported on resins and promote the photo-Fenton reaction under visible irradiation (*19*−*22*). To study whether the decomposition of H_2O_2 can be promoted via photoassisted reduction of structural Fe(III) by photoreactive organic species, the variation in H_2O_2 concentration in C-MK10/organic system was examined under UV or visible irradiation. Considering the low redox potential of MG/RhB/DMA excited states (−1.08 V, −1.09 V and 2.85 V vs NHE) (*22*, *39*, *40*) and their affinity to clay particles, they were selected as the potential electron donors to structural Fe(III) (∼0.44 V vs NHE) (*41*). As displayed in Figure 3 (curve a), addition of DMA, RhB, or MG accelerates significantly H_2O_2 decomposition in the presence of C-MK10 under light irradiation. In reaction systems merely containing these organics, however, the decomposition of H_2O_2 was much slower (curve b). Organics such as cetyltrimethylammonium bromide (CTAB), which also intercalates into the clay layer but cannot be excited by irradiation above 300 nm and donate electrons to Fe(III), did not accelerate the decomposition of H_2O_2 (Supporting Information, Figure S3). In addition, in comparison with C-MK10, iron free Laponite had insignificant impact on decomposition of H_2O_2 (Supporting Information, Figure S4), indicating that structural Fe(III) in C-MK10 is essential to trigger the overall reaction. In other words, it acts as the electron relay between excited organics and H_2O_2.

The interaction between excited organics and clay was further examined by fluorescence measurements. Figure S5 displays the influence of H_2O_2 and C-MK10 on the fluorescence emission spectra of RhB. The 50 μM H_2O_2 had insignificant effect on the fluorescence of RhB. However, C-MK10 at a concentration of 0.04 g/L efficiently quenched it. The quenching of RhB fluorescence by C-MK10 was indirect evidence for the electron transfer between RhB and C-MK10. Besides, upon introduction of the DMA, RhB, and MG, the production of Fe(II) in H_2O_2-free C-MK10 dispersions increased obviously (Table 1), confirming that these organics donate electrons to structural Fe(III) under light irradiation.

Contribution of Solution Phase Reaction to the Decomposition of H_2O_2. To understand the role of dissolved iron in the decomposition of H_2O_2, dispersions of MK10 and C-MK10/RhB (clay, 0.2 g/L; RhB, 2.0 × 10^{-5} M) were irradiated first for 4 h; subsequently, they were centrifuged and the supernatants were collected (*42*). Then H_2O_2 was added to

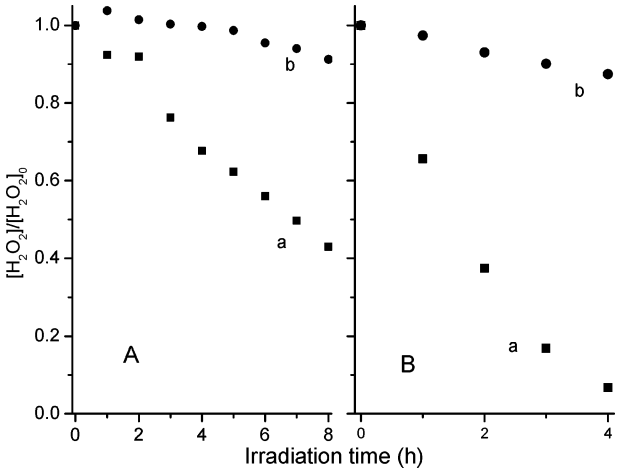

FIGURE 4. Variation in H_2O_2 concentration (a) in the dispersion and (b) the supernatants after irradiation and the following centrifugation. Key: (A) 0.2 g/L MK10, under UV irradiation; (B) 0.2 g/L C-MK10 and 2.0×10^{-5} M RhB, under visible irradiation. The initial concentration of H_2O_2 was 40 μM, and pH = 5.0.

the supernatants and the variation in H_2O_2 concentration was monitored. As displayed in Figure 4, the decrease in H_2O_2 concentration was less than 10% in MK10 supernatants with 8 h of UV irradiation, much less than that in MK10 dispersion. In C-MK10/RhB supernatants, the rate of H_2O_2 also decreased greatly in the centrifuged solution: only 13% of H_2O_2 was decomposed, while, in C-MK10/RhB dispersion, 94% of H_2O_2 was decomposed with 4 h of irradiation. In addition, in the kinetic study of H_2O_2 decomposition, the dissolved iron before and after reaction was also measured in dispersions of MK10, C-MK10, and CMK10/RhB (Supporting Information, Table S2). Despite the quite different rates of H_2O_2 decomposition in these systems, the concentration of total dissolved iron in all these systems was at low level and did not vary significantly during the reaction, demonstrating that the reaction primarily localized on the clay surface.

Measurement of Hydroxyl Radical in Clay-Catalyzed H_2O_2 Decomposition. The EPR technique using DMPO as the trapping reagent was employed to detect the generation of hydroxyl radical (•OH) in various irradiated systems. The results are displayed in Figure 5. The signal of DMPO−•OH adducts characterized by intensity ratio of 1:2:2:1 was observed in the MK10/H_2O_2 system and increased upon 355 nm laser irradiation. After the free iron oxides were removed, no signal could be detected (Figure 5B), consistent with the poor activity of structural Fe(III) to catalyze H_2O_2 decomposition.

Structural iron greatly accelerated the decomposition of H_2O_2 in the presence of DMA, RhB, or MG under UV/visible irradiation. The above experiment results implied that these organics assist H_2O_2 decomposition by reducing structural Fe(III) to Fe(II). But the signal of DMPO−•OH was hardly observed in these systems under 355 or 532 nm laser irradiation (Figure 6). However, in clay-contained structural Fe(II) (*43*), the signal of •OH was detected (Supporting Information, Figure S6). The inconsistency might result from

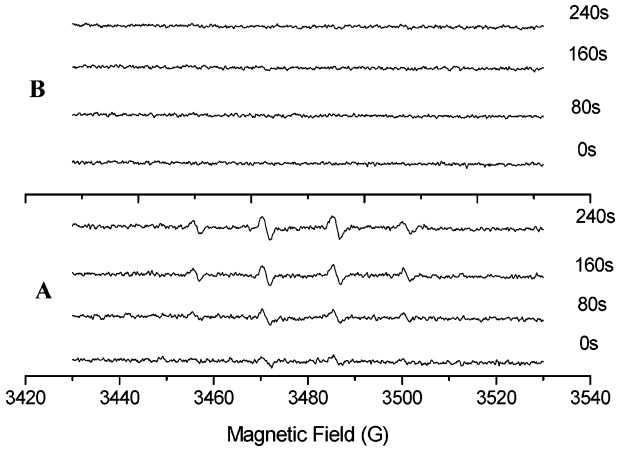

FIGURE 5. DMPO spin-trapping EPR spectra of aqueous H_2O_2 (1.0×10^{-4} M) solution in the presence of 1 g/L (A) MK10 and (B) C-MK10 (355 nm laser irradiation).

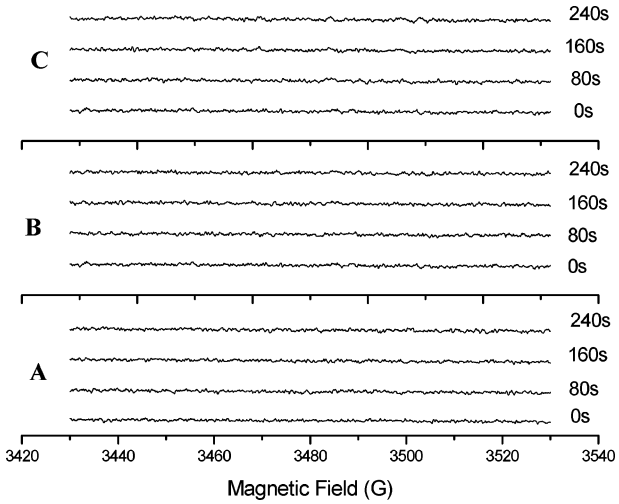

FIGURE 6. DMPO spin-trapping EPR spectra of the reaction systems containing 1 g/L C-MK10 and 1.0×10^{-4} M H_2O_2 for (A) 1.0×10^{-4} M DMA, (B) 2.0×10^{-5} M RhB, and (C) 4.0×10^{-5} M MG. Irradiation source: (A) 355 nm laser; (B, C) 532 nm laser.

the competition between organics and spin trapper DMPO for •OH. Despite the concentration of the photoreactive organics being lower than that of DMPO (0.01 M), they could react rapidly with •OH (*44*) and they have great affinity to clay particles: RhB, MG, and DMA were ready to adsorb on clay; their characteristic absorption peaks in the solution phase almost disappeared within several minutes. As a consequence, the generated •OH was consumed rapidly by the adsorbed organics before being trapped by DMPO in solution. Other reactive intermediates may also be produced during the decomposition of H_2O_2 and need further identification.

Scheme 1 gives simplified pathways of H_2O_2 decomposition catalyzed by iron-bearing clay. Under UV light irradiation, surface Fe(II) species are formed through the photolysis of free iron oxides in clay. The speedy reaction between Fe(II)

SCHEME 1. Proposed Route of H_2O_2 Decomposition Catalyzed by Iron Oxides and Structural Iron in the Presence of Photoreactive Substances

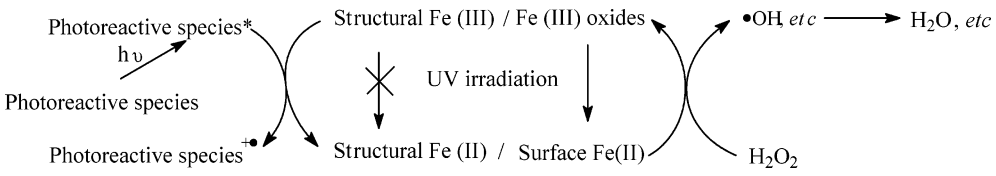

and H_2O_2 results in the reoxidation of Fe(II), as well as the decomposition of H_2O_2. Structural Fe(III) in an octahedral lattice, however, could hardly be reduced to structural Fe(II) under the same conditions. As a result, it shows poor reactivity to catalyze the decomposition of H_2O_2. Introduction of photoreactive organics, which are able to donate electrons to structural iron after being excited or reduce structural Fe(III) to Fe(II) via other electron transfer pathways, promotes greatly this process under UV or visible irradiation. The photoinduced Fe(III)/Fe(II) redox cycling does not caused significant release of iron to the solution phase, and the decomposition of H_2O_2 primarily takes place on the clay surface. The clay-catalyzed decomposition of H_2O_2 is accompanied by the generation of reactive oxygen species such as hydroxyl radical, indicating that iron-bearing clays could be promising catalysts in remediation of polluted water.

In summary, iron-bearing clay could contribute to the decay of environmental H_2O_2 via the photochemical cycling of iron species under particular conditions. Fe(III) in free iron oxides can be directly reduced to Fe(II) upon UV irradiation through LMCT reaction, and the dominant structural Fe(III) in the octahedral lattice of clay could be reduced to Fe(II) by photoreactive organics under light irradiation, leading to the decomposition of H_2O_2 and the simultaneous transformation of inorganic or organic matters attached to clay.

Acknowledgments

This work was financially supported under grants from the Ministry of Science and Technology of China (No. 2003CB-415006), the Natural Science Foundation of China (Nos. 20520120221, 20537010, and 20407016), and the Chinese Academy of Sciences.

Supporting Information Available

Content of iron in each clay sample, calculation of the free oxide amount in clay, cyclic decomposition of H_2O_2 in the presence of 0.2 g/L MK10 under UV irradiation, effect of phosphate and EDTA on decomposition of H_2O_2 in the presence of MK10, effect of cetyltrimethylammonium bromide on the decomposition of H_2O_2 in the presence of C-MK10, variation of H_2O_2 in the presence of laponite and photoreactive organic species, effect of MK10 and H_2O_2 on fluorescence of RhB, and measurement of dissolved iron before and after photoreaction in dispersion of MK10, C-MK10, and CMK10/RhB ($H_2O_2 = 40\ \mu M$, pH = 5.0). This material is available free of charge via the Internet at http://pubs.acs.org.

Literature Cited

(1) Kok, G. L. Measurements of hydrogen peroxide in rainwater. *Atmos. Environ.* **1980**, *653*, 653−656.
(2) Faust, B. C.; Anastasio, C.; Allen, J. M.; Arakaki, T. Aqueous-phase photochemical formation of peroxides in authentic cloud and fogwaters. *Science* **1993**, *260*, 73−75.
(3) Wilson, C. L.; Hinman, N. W.; Cooper, W. J.; Brown, C. F. Hydrogen peroxide cycling in surface geothermal waters of Yellowstone National Park. *Environ. Sci. Technol.* **2000**, *34*, 2655−2662.
(4) Voelker, B. M.; Sulzberger, B. Iron redox cycling in surface waters: effects of humic substances and light. *Environ. Sci. Technol.* **1997**, *31*, 1004−1011.
(5) Zuo, Y. G.; Holgné, J. Formation of hydrogen peroxide and depletion of oxalic acid in atmospheric water by photolysis of iron (III)−oxalato complexes. *Environ. Sci. Technol.* **1992**, *26*, 1014−1022.
(6) Hug, S. J.; Leupin, O. Iron-catalyzed oxidation of arsenic(III) by oxygen and by hydrogen peroxide: pH-dependent formation of oxidants in the Fenton reaction. *Environ. Sci. Technol.* **2003**, *37*, 2734−2742.
(7) Kwan, W. P.; Voelker, B. M. Decomposition of hydrogen peroxide and organic compounds in the presence of dissolved iron and ferrihydrite. *Environ. Sci. Technol.* **2002**, *36*, 1467−1476.
(8) Kwan, W.; Volker, B. M. Rates of hydroxyl radical generation and organic compound oxidation in mineral-catalyzed Fenton-like systems. *Environ. Sci. Technol.* **2003**, *37*, 1150−1158.
(9) Petigara, B. R.; Blough N. V.; Mignerey, A. C. Mechanisms of hydrogen peroxide decomposition in soils. *Environ. Sci. Technol.* **2002**, *36*, 639−645.
(10) Lin, S. S.; Gurol, M. D. Catalytic decomposition of hydrogen peroxide on iron oxide: kinetics, mechanism, and implications. *Environ. Sci. Technol.* **1998**, *32* (10), 1417−1423.
(11) Watts, R. J.; Foget, M. K.; Kong, S.-H.; Teel, A. L. Hydrogen peroxide decomposition in model subsurface systems. *J. Hazard. Mater.* **1999**, *69*, 229−243.
(12) Paciolla, M. D.; Davies, G.; Jansen, S. Generation of hydroxyl radicals from metal-loaded humic acids. *Environ. Sci. Technol.* **1999**, *33*, 1814−1818.
(13) Faust, B. C.; Hoffmann, M. R. Photoinduced reductive dissolution of α-Fe_2O_3 by bisulfite. *Environ. Sci. Technol.* **1984**, *20*, 943−948.
(14) Lopes, L.; Laat, J.; Legube, B. Charge transfer of iron(III) monomeric and oligomeric aqua hydroxo complexes: Semiempirical investigation into photoactivity. *Inorg. Chem.* **2002**, *41*, 2505−2517.
(15) Nadtochenko, V. A.; Kiwi, J. Photolysis of $FeOH_2^+$ and $FeCl_2^+$ in aqueous solution. photodissociation kinetics and quantum yields. *Inorg. Chem.* **1998**, *37*, 5233−5238.
(16) Southworth, B. A.; Voelker, B. M. Hydroxyl radical production via the photo-Fenton reaction in the presence of fulvic acid. *Environ. Sci. Technol.* **2003**, *37*, 1130−1136.
(17) Gaberell, M.; Chin, Y.-P.; Hug, S. J.; Sulzberger, B. Role of dissolved organic matter composition on the photoreduction of Cr(VI) to Cr(III) in the presence of iron. *Environ. Sci. Technol.* **2003**, *37*, 4403−4409.
(18) Song, W. J.; Ma, W. H.; Ma, J. H.; Chen, C. C.; Zhao, J. C.; Xu, Y. M.; Huang, Y. P. Photochemcial oscillation of Fe(II)/Fe(III) induced by periodic flux of dissolved organic matter. *Environ. Sci. Technol.* **2005**, *39*, 3121−3127.
(19) Chen, F.; Ma, W. H.; He, J. J.; Zhao, J. C. Fenton degradation of malachite green catalyzed by aromatic additives. *J. Phys. Chem. A* **2002**, *106*, 9485−9490.
(20) Ma, J. H.; Song, W. J.; Chen, C. C.; Ma, W. H.; Zhao, J. C.; Tang, Y. L. Fenton degradation of organic compounds promoted by dyes under visible irradiation. *Environ. Sci. Technol.* **2005**, *39*, 5810−5815.
(21) Cheng, M. M.; Ma, W. H.; Li, J.; Huang, Y. P.; Zhao, J. C. Visible light-assisted degradation of dye pollutants over Fe(III)-loaded resin in the presence of H_2O_2 at neutral pH values. *Environ. Sci. Technol.* **2004**, *38*, 1569−1575.
(22) Wu, K. Q.; Xie, Y. D.; Zhao, J. C.; Hidaka, H. Photo-Fenton degradation of a dye under visible irradiation. *J. Mol. Catal.* **1999**, *144*, 77−84.
(23) Shichi, T.; Takagi, K. Clay minerals as photochemical reaction fields. *J. Photochem. Photobiol., C: Photochem. Rev.* **2000**, *1*, 113−130.
(24) Thomas, J. K. Physical aspects of radiation-induced processes on SiO_2, −Al_2O_3, zeolites, and clays. *Chem. Rev.* **2005**, *105*, 1683−1734.
(25) Cervini-Silva, J. Coupled hydrophilic and charge-transfer interactions between polychlorinated methanes, ethanes, and ethenes and redo-manipulated smectite clay minerals. *Langmuir* **2004**, *20*, 9878−9881.
(26) Kostka, J. E.; Haefele, E.; Viehweger, R.; Stucki, J. W. Respiration and dissolution of iron(III)-containing clay minerals by bacterica. *Environ. Sci. Technol.* **1999**, *33*, 3127−3133.
(27) Hofstetter, T. B.; Schwarzenbach, R. P.; Haderlein, S. B. Reactivity of Fe(II) species associated with clay minerals. *Environ. Sci. Technol.* **2003**, *37*, 519−528.
(28) Elsner, M.; Schwarzenbach, R. P.; Haderlein, S. B. Reactivity of Fe(II)-bearing minerals toward reductive transformation of organic contaminants. *Environ. Sci. Technol.* **2004**, *38*, 799−807.
(29) Zen, J. M.; Jeng, S. H.; Chen, H. J. Catalysis of the electroreduction of hydrogen peroxide by nontronite clay coatings on glassy carbon electrodes. *J. Electroanal. Chem.* **1996**, *408*, 157−163.
(30) Zen, J. M.; Lo, C. W. A Glucose sensor made of an enzymatic clay-modified electrode and methyl viologen mediator. *Anal. Chem.* **1996**, *68*, 2635−2640.
(31) Pignon, F.; Alemdar, A.; Magnin, A.; Narayanan, T. Small-angle X-ray scattering studies of Fe-montmorillonite capacity is negilibldeposits during ultrafiltration in a magnetic field. *Langmuir* **2003**, *19*, 8638−8645.

(32) Ghosh, P. K.; Bard, A. J. Photochemistry of tris(2,2′-bipyridyl)-ruthenium(II) in colloidal clay suspensions. *J. Phys. Chem.* **1984**, *88*, 5519−5526.

(33) Bander, H.; Sturzenegger, V.; Hoigné. J. Photometric method for the etermination of low concentrations of hydrogen peroxide by the peroxidase catalyzed oxidation of N,N-diethyl-*p*-phenylenediamine (DPD). *Water Res.* **1988**, *22*, 1109−1115.

(34) Stookey, L. L. Ferrozine-A New Spectrophotometric Reagent for Iron. *Anal. Chem.* **1970**, *42*, 779−781.

(35) Kari, F. G.; Hilger, S.; Canonica, S. Determination of the reaction quantum yield for the photochemical degradation of Fe(III)−EDTA: Implications for the environmental fate of EDTA in surface waters. *Environ. Sci. Technol.* **1995**, *29*, 1008−1017.

(36) Schultz, S. A.; Grundl, T. J. PH dependence on reduction rate of 4-Cl-nitrobenzene by Fe(II) montmorillonite systems. *Environ. Sci. Technol.* **2000**, *34*, 3641−3648.

(37) He, J.; Ma, W. H.; Song, W. J.; Zhao, J. C.; Qian, X. H.; Zhang, S. B.; Yu, J. C. Photoreaction of aromatic compounds at α-FeOOH/H_2O interface in the presence of H_2O_2: evidence for organic-goethite surface complex formation. *Water Res.* **2005**, *39*, 119−128.

(38) Borer, P. M.; Sulzberger, B.; Reichard, P.; Kraemer, S. M. Effect of siderophores on the light-induced dissolution of colloidal iron(III) (hydr)oxides. *Mar. Chem.* **2005**, *93*, 179−193.

(39) Takizawa, T.; Watanabe T.; Honda, K. Photocatalysis through excitation of adsorbates. 2. a comparative study of rhodamine B and methylene blue on cadmium sulfide. *J. Phys. Chem.* **1978**, *82*, 1391−1396.

(40) Banerjee, A.; Falvey, D. E. Protecting groups that can be removed through photochemical electron transfer: mechanistic and product studies on photosensitized release of carboxylates from phenacyl esters. *J. Org. Chem.* **1997**, *62*, 2, 6245−6251.

(41) Swearingen, C.; Wu, J.; Stucki, J.; Fitch A. Use of ferrocenyl surfactants of varying chain lengths to study electron-transfer reactions in native montmorillonite clay. *Environ. Sci. Technol.* **2004**, *38*, 5598−5603.

(42) Since RhB was adsorbed by clay particles, 2.0×10^{-5} M RhB was added to the supernatants after centrifugation, in which the H_2O_2 decomposition was examined.

(43) Preparation of clay-containing structural Fe(II): MK10 was treated with the CBD method, during which structural Fe(III) was reduced to structural Fe(II). Then it was washed and freeze-dried to avoid the reoxidation of Fe(II).

(44) The rate constants of reactions between •OH and DMPO, RhB, and DMA are 4.3×10^9, 2.5×10^{10}, and 1.4×10^{10} $L \cdot mol^{-1} \cdot s^{-1}$. Data are from the Radiation Chemistry Data Center of the Notre Dame Radiation Laboratory, www.rcdc.nd.edu/compilations/Hydroxyl/OH.htm.

Received for review March 16, 2006. Revised manuscript received May 16, 2006. Accepted June 1, 2006.

ES060624Q